

Least-Squares Fitting Method for On-Line Flux mapping of CANDU-PHWR

In Seob Hong and Chang Hyo Kim

Nuclear Engineering Department, Seoul National University
San 56-1, Shillim-dong, Kwanak-ku, Seoul 151-742, Republic of Korea

Ho Chun Suk

Korea Atomic Energy Research Institute
150 Dukjin, Yusong, Daejeon 305-353, Republic of Korea

Abstract

A least-squares fitting method is developed for advanced on-line flux mapping in the CANDU-PHWR system. The method solves both the core neutronics design equations and the detector response equations on the least-squares principle which leads one to normal equations. The fine-mesh finite difference two-group diffusion theory calculations by SCAN code for Wolsong-3 unit are conducted to obtain the simulated real flux distribution and detector signals. The least-squares flux monitoring calculations are compared with the flux distribution calculation by the SCAN code without detector signals. It is shown that the least-squares method produces the flux distribution in better agreement with reference distribution than the coarse mesh SCAN calculation without detector signals. Through the 500 full power day burnup-history simulations of Wolsong-4 unit for benchmark, the mapped detector signals are compared with real detector signals. Maximum root mean squares (RMS) difference between the mapped detector signals and real detector signals are shown to be about 0.04 % by least-squares method, while it is about 5.43 % by the current flux-synthesis method. It is concluded that the least-squares fitting method is very promising as the advanced flux mapping methodology for CANDU-PHWR.

1. Introduction

The current on-line flux mapping system of CANDU designs is based on flux synthesis method¹⁻³⁾ in which the three-dimensional flux distribution in the reactor is

assumed by a linear combination of a number of pre-calculated flux modes and the amplitudes of the modes are determined by a least-squares fit of the calculated fluxes at the 102 vanadium in-core detectors to the measured fluxes. This method is very fast, yet it suffers a few deficiencies. It requires pre-calculated modes. Because of this, it cannot take into account the complete core operation history for the flux or the power distributions. It does not provide local power distributions as accurate as desired. Improved methods aimed at overcoming these deficiencies have been proposed^{4, 5)}. The purpose of this paper is to present a new method that makes the direct use of the core neutronics design equations and the detector response equations on the least-squares fitting principle and to demonstrate that the new method can result in the improved flux mapping in accuracy by performing the flux mapping calculations using simulated detector signals through the fine-mesh neutronics calculations and the vanadium in-core detector signals measured at Wolsong CANDU reactor units. The new method is implemented into the SCAN (Seoul National University CANDU-PHWR Neutronics) code, which is introduced at last conference paper⁶⁾.

2. Least-Squares Fitting Method

The new least-squares fitting method for the improved flux mapping in the CANDU reactor solves the steady-state, two-group diffusion equations,

$$\mathbf{M}\Phi = \frac{1}{\lambda} \mathbf{F}\Phi \quad (1)$$

and the in-core detector response equations,

$$\mathbf{D}\Phi = \mathbf{s} \quad (2)$$

Φ is a NG -dimensional flux vector in which N is the number of spatial meshes and G the number of groups – two in this problem. \mathbf{M} and \mathbf{F} are $NG \times NG$ square matrices representing destruction and production of neutrons, respectively. \mathbf{D} is $N_d G \times NG$ matrix in which N_d denotes the number of the in-core detectors.

The two equations (1) and (2) can be put together in the matrix form,

$$\begin{pmatrix} \mathbf{M} & -\frac{1}{\lambda} \mathbf{F} \\ & \mathbf{D} \end{pmatrix} \Phi = \begin{pmatrix} \mathbf{0} \\ \mathbf{s} \end{pmatrix} \quad \text{or} \quad \mathbf{A}\Phi = \mathbf{b} \quad (3)$$

The equation (3) is an over-determined system of equations in which the number of equations, i.e., $(N+N_d)G$, is greater than that of the unknowns, NG . Because of this, it is

not generally possible to find Φ that satisfies Eq. (3). Instead, one finds the least-squares solution to Eq. (3), which can be obtained by solving so-called normal equations.

$$\mathbf{A}^T \mathbf{A} \Phi = \mathbf{A}^T \mathbf{b} \quad (4)$$

Note that the normal equations are derived from minimizing the L_2 norm of $\mathbf{A}\Phi - \mathbf{b}$, the solution of which produce flux-mapped fluxes that lies in between computed fluxes and real on-line detected fluxes. \mathbf{A}^T is the transpose of the matrix \mathbf{A} . Many different solution methods of the normal equations are available in reference 7. We found the conjugate gradient method is the most effective in terms of computing time. And diagonal preconditioning⁷⁾ and bi-diagonal QR preconditioning^{8,9)} are applied to achieve faster convergence of above normal equations.

At this point, a little discussion need be made on the detector response equations. In the current CANDU neutronics method based on the finite-difference diffusion theory equations, the unknowns in Eq. (1) are the two-group fluxes at the centers of the unit cells each of which consists of fuel bundle and associated moderator. Because the vanadium detectors are located in moderator, the current reading of a vanadium detector gives the flux information at the site of the detector instead of the information on the unknowns in equation (1). To derive detector response equations (2), therefore, we assumed that the flux at a detector can be obtained by interpolation of the unknown thermal fluxes of the unit cells surrounding the detector. With this assumption, we represent each detector signal by

$$S_d = \sum_{p=1} W_p \Phi_2^p ; d=1,2, \dots, N_d \quad (5)$$

where S_d is signal of detector ($d=1,2, N_d$), W_p the weighting factor of Lagrange interpolation of 1st, 2nd or 3rd orders, p is the index of neighbor mesh and Φ_2^p thermal flux of unit cell p . The summation over p runs through all the unit cells employed in the interpolation. Figure 1 shows a sample configuration of a detector unit and its neighbor meshes for the 1st order interpolation, which uses 8 neighbor meshes' information.

3. Numerical Results and Discussion

We examined the applicability of the above least-squares formulation for the improved flux mapping in the Wolsong-3 CANDU reactor. The vanadium detector measurements and the flux mapping results from the Wolsong-3 plant can be utilized in this examination. Table 1 shows the conditions used in the examination. Before using

them directly, we generated the reference bundle power distribution for Wosung-3 core by a fine-mesh finite difference two-group diffusion theory calculation by SCAN code, CANDU Neutronics Analysis Code of Seoul National University⁶⁾. For the fine-mesh reference calculation, the single unit cell adopted for the routine neutronics calculations in the RFSP code³⁾ is divided into 64 (=4x4x4) fine mesh cells. Considering that the RFSP calculation routinely adopt 42x34x20 coarse mesh cells, the number of fine-mesh cells in the reference fine-mesh calculation is 64 times the number of the coarse mesh cells. The fine-mesh reference calculation is also used to generate the simulated detector signals through Lagrange interpolation. Table 2 compares the simulated detector signals generated by 42x34x20 coarse-mesh interpolation of 1st, 2nd and 3rd orders with the corresponding reference fine-mesh interpolation results. We can observe that detector signals generated by interpolation of 1st, 2nd and 3rd orders are similar between each other and that the interpolation of 1st order is enough for the generation of detector signals. The reference fine-mesh results for bundle and channel powers as well as the simulated detector signals are then presumed to be real. Table 3 shows a comparison of the maximum channel and bundle powers predicted by the least-squares flux mapping calculations and the ordinary core neutronics calculations without use of simulated detector signals on the routine 42x34x20 mesh configuration by the SCAN code. It is noted that the least-squares flux mapping predicts the maximum bundle and channel powers more closely than the ordinary core neutronics calculation that does not utilize the detector signals. From the standpoint of computing time, the least-squares method takes longer computing time. The last two-columns show that preconditioning of the conjugate gradient methods can save the computing time of the least-squares flux mapping calculation. Figure 2 shows the convergence characteristics using preconditioners.

For further examination, we carried out core depletion calculation to 500 effective full power days and flux-mapping calculations at a number of discrete core burnup steps for Wolsong-4. Table 4 compares the maximum bundle powers at several different effective full power days in the Wolsong-4 from the two flux-mapping methods, the least-squares method implemented in the SCAN code and the current synthesis method. Table 5 and Figure 3 compares the difference between the actual vanadium flux signals and the estimated detector thermal fluxes in the Wolsong-4. Because the true bundle powers are not known, there is no way of knowing the superiority of one method over the other in prediction accuracy. Yet Table 5 and Figure 3 clearly shows that the proposed least-squares method is advantageous because the mapped detector flux signals from it are closer to the actual detector flux signals than those from the current synthesis method.

The above results demonstrate that the least-squares fitting method is very promising as the advanced flux mapping methodology. Besides being accurate, it has more advantages than the synthesis method in that it does not need the pre-calculation of equations that is necessary in the synthesis method.

References

1. E. Hinchley and G. Kugler, "On-Line Control of the CANDU-PHW Power Distribution", IAEA Specialists Meeting on Spatial Control Problems, Studsvik, Sweden, October (1974).
2. T.L. Tang., et al., "Analytical Design of the CANDU-600 On-Line FLux Mapping System", TDAI-152, AECL (1978).
3. D.A. Jenkins, B. Rouben, "Reactor Fuelling Simulation Program - RFSP: User's Manual for Microcomputer Version", TTR-321, AECL (1978).
4. P.S.W. Chan and M. Mamourian, "Application of On-Line Solution of 3-Dimensional Multigroup Finite-Difference Neutron Diffusion Equations in Reactor Power Control System", 3rd International Conference on Simulation Methods in Nuclear Engineering, April 18-20, Montreal, Quebec, (1990).
5. B.G. Kim, I.S. Kim, S.Y. Kim, "Core Simulation Using Actual Detector Readings for CANDU Reactors", Nuclear Technology 93, 138 (1991).
6. I.S. Hong, C.H. Kim, B.J. Min and H.C. Suk, "Development of CANDU-PHWR Neutronics Code SCAN", Proceedings of Seventh International Conference on CANDU Fuel, Vol 1, pp77~86, CANADA, September 2001.
7. Youseff Saad. "Iterative Methods for Sparse Linear Systems", University of Minnesota, PWS Publishing Company(1996).
8. X. Wang, K. A. Gallivan, and R. Bramley, "CIMGS: An Incomplete Orthogonal Factorization Preconditioner", Tech. Rep. 393, Department of Computer Science, Indiana University, Bloomington, IN 47405, 1993.
9. T. Yang. "Data Distribution and Communication Schemes for Least Squares Problems on Massively Distributed Memory Computers", Department of Computer Science, Linköping University, Sweden, September 13, 1996.

Table 1 Numerical Simulation Benchmark Condition from Phase-B Simulation of Wolsong Unit 3

Variable	Value
Boron Concentration(ppm)	9
Moderator Temp(K)	310.10
Coolant,Fuel Temp(K)	305.31
Moderator Purity(w%)	99.81
Coolant Purity(w%)	99.24
Device Condition	Normal (ADJ in, MCA out, SOR out)

Table 2 Detector Signal Vs Interpolation Order (Wolsong Unit 3)

Mesh model		64 nodes / 1 n 1 st order Reference	42x34x20 1 st order	42x34x20 2 nd order	42x34x20 3 rd order
Interpolated detector thermal flux diff [%]	ϵ_{\max}	-	6.03	6.66	6.47
	ϵ_{avg}	-	1.26	1.09	1.12
Mesh model		64 nodes / 1 n 2 nd order Reference	42x34x20 1 st order	42x34x20 2 nd order	42x34x20 3 rd order
Interpolated detector thermal flux diff [%]	ϵ_{\max}	-	5.86	6.49	6.31
	ϵ_{avg}	-	1.23	1.10	1.12
Mesh model		64 nodes / 1 n 3 rd order Reference	42x34x20 1 st order	42x34x20 2 nd order	42x34x20 3 rd order
Interpolated detector thermal flux diff [%]	ϵ_{\max}	-	5.84	6.47	6.29
	ϵ_{avg}	-	1.24	1.09	1.11

Table 3 Comparison of Ordinary Neutronics Calculation without Use of Detector Signals and Least Squares Flux Mapping Calculation

Method	Reference	Without use of detector signals	Least Squares using detector signals	Least Squares with Diagonal Precondition	Least Squares with Bi-diagonal QR Precondition	
Mesh Configuration	168×136×80	42×34×20	42×34×20	42×34×20	42×34×20	
Number of iterations	-	84(1)	84 + 529(2)	84 + 270	84 + 164	
5 Maximum channel power[W] and position	6973 (O06)	6975 (O06)	6977 (F08)	6977 (F08)	6977 (F08)	
	6972 (N05)	6958 (O17)	6973 (F15)	6973 (F15)	6973 (F15)	
	6963 (O17)	6951 (F08)	6968 (O06)	6968 (O06)	6970 (O06)	
	6959 (N18)	6947 (N06)	6960 (O17)	6960 (O17)	6962 (O17)	
	6958 (M05)	6943 (N05)	6947 (N05)	6948 (N05)	6950 (N05)	
5 Maximum bundle power[W] and position	789 (E12 07)	780 (D12 07)	789 (D12 07)	789 (D12 07)	789 (D12 07)	
	788 (E11 07)	779 (D11 07)	788 (D11 07)	788 (D11 07)	788 (D11 07)	
	787 (E11 06)	779 (E12 07)	788 (D11 06)	788 (D11 06)	788 (D11 06)	
	786 (D12 07)	778 (D11 06)	787 (D12 06)	787 (D12 06)	787 (D12 06)	
	786 (D11 07)	778 (E11 07)	784 (E12 07)	784 (E12 07)	784 (E12 07)	
Channel power diff [%]	ϵ_{\max} (position)	-	5.76 (O22)	3.93 (O22)	3.95 (O22)	4.11 (O22)
	ϵ_{avg}	-	1.17	0.73	0.73	0.74
CPU TIME(3) [sec]		-	1.80	6.63	4.91	4.60

(1) Ordinary neutronics calculation without use of detector signals

(2) Number of (SOR/Chebyshev) outer iteration + number of (CGNR) inner iteration

(3) CPU Time on P4. 1.8GHz PC

Table 4 Maximum Channel Powers from Two Flux-Map Calculations :
Least Squares Method and Flux Synthesis Method

FPD (Full Power Days)	Max Channel Power [Kw] and Position		
	SCAN	Flux Synthesis Method	Difference [%]
49	6846 O06	6820 O17	0.38
101	6585 P07	6543 O06	0.64
197	6905 P11	6856 P11	0.71
298	6891 Q08	6887 O06	0.06
399	6991 Q08	6956 Q08	0.50
486	6986 R15	6926 P07	0.87

Table 5 Comparison of Differences from Real Detector Flux Signals and Flux Signals
Mapped by Least Squares Method and Flux Synthesis Method

FPD (Full Power Days)	RMS Difference [%]		MAX Difference [%]	
	SCAN	Flux Synthesis Method	SCAN	Flux Synthesis Method
49	0.03	1.70	0.15	-4.44
101	0.03	1.62	0.10	-5.03
197	0.04	1.76	0.15	3.81
298	0.03	1.76	-0.09	4.38
399	0.04	1.82	0.10	5.43
486	0.04	1.97	0.12	-5.13

Figure 1 Configuration of a Detector Unit and Neighbor Meshes

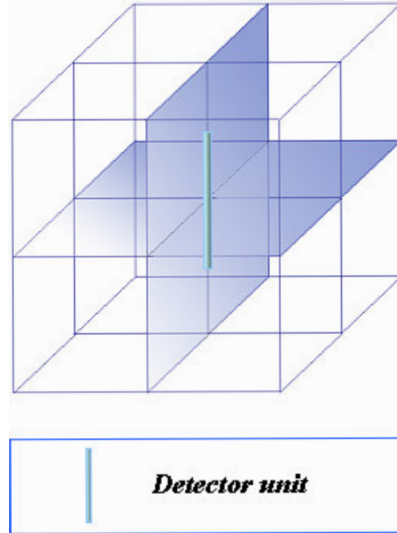


Figure 2 Convergence Characteristics of Numerical Methods

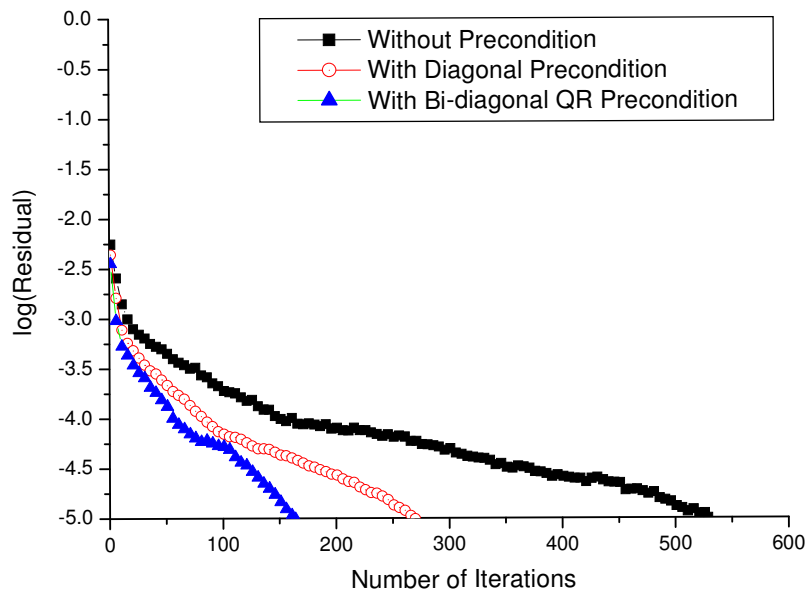
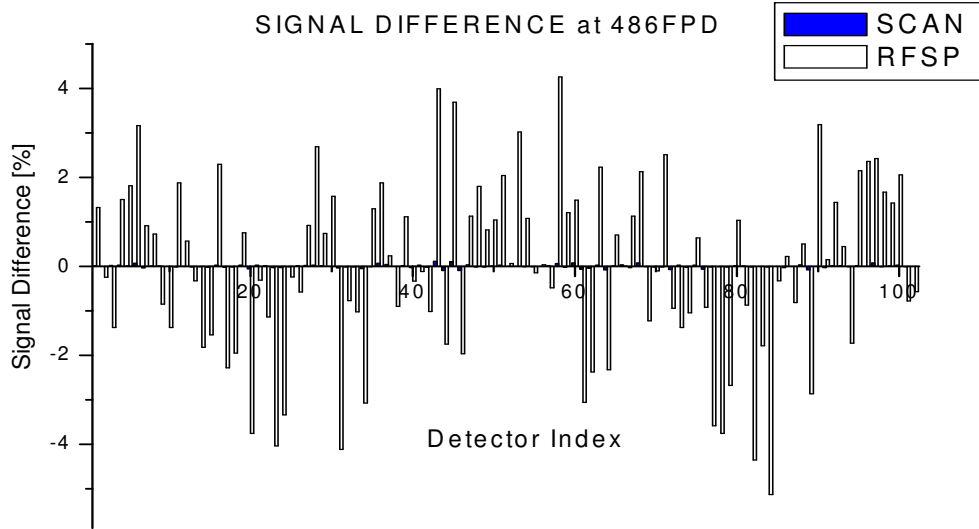


Figure 3 Difference Estimation between Real Detector Flux Signals and Mapped Flux Signals (486FPD of Wolsong Unit 4)



- SCAN RMS DIFFERENCE = 0.04 %

- RFSP RMS DIFFERENCE = 1.97 %